

Non-classical properties of quantum wave packets propagating in a Kerr-like medium

C. Sudheesh, S. Lakshimbala, and V. Balakrishnan*

Department of Physics, Indian Institute of Technology Madras, Chennai 600 036, India

(Dated: October 30, 2018)

We investigate non-classical effects such as fractional revivals, squeezing and higher-order squeezing of photon-added coherent states propagating through a Kerr-like medium. The Wigner functions corresponding to these states at the instants of fractional revivals are obtained, and the extent of non-classicality quantified.

PACS numbers: 03.65.-w, 42.50.-p, 42.50.Md, 42.50.Dv

Keywords: Photon-added coherent states, fractional revivals, higher-order squeezing, Wigner function.

I. INTRODUCTION

Non-classical effects such as revivals and squeezing exhibited by quantum wave packets while propagating through different media are of great interest in the context of quantum information processing with continuous variables[1]. Both the nature of the medium in which the state propagates and the precise initial state considered play a crucial role in determining the subsequent dynamics of the state. With the experimental realization of several non-classical states in quantum optics[2], it has become important to examine more closely their dynamical properties. Detailed investigations have been carried out, for instance, on the revival phenomena displayed by an initial coherent state evolving under different Hamiltonians[3]. In particular, the non-classical features displayed by a wave packet which is initially a coherent state while it propagates through a nonlinear, Kerr-like medium have been examined. Its squeezing and higher-order squeezing properties have been discussed[4], and signatures of wave packet revivals and fractional revivals have been shown to be captured in the expectation values of appropriate observables [5].

In this paper, we examine the effects of the *departure* from coherence of the initial state on the subsequent non-classical features it displays while evolving in a Kerr-like medium. In order to be able to compare with exactitude these effects with those that arise in the dynamics of an initial coherent state (CS), it is essential to consider such initial states as display a precisely quantifiable departure from coherence. The photon-added coherent states (PACS) are promising candidates for this purpose [6]. We examine a spectrum of non-classical phenomena such as revivals, fractional revivals, squeezing and higher-order squeezing displayed by an initial PACS as it propagates in a Kerr-like medium, and identify the effects arising from the departure from perfect coherence of the initial state.

The plan of the paper is as follows: In the next section, we review briefly the salient features of revivals and fractional revivals of a wave packet, and identify quan-

tifiers which provide signatures to distinguish between fractional revivals of initial wave packets that are ideal CS from those that are PACS. In Section III, we examine the dependence of squeezing and higher-order squeezing effects on the extent of coherence of the initial wave packet. In the final section, we estimate the degree of non-classicality displayed by a CS and by a PACS at specific instants while evolving in a Kerr-like medium, by quantifying the extent of negativity of the corresponding Wigner functions.

II. WAVE PACKET REVIVALS

A wave packet propagating through a nonlinear medium may display revivals and fractional revivals at specific instants of time. In the one-dimensional case, if the initial wave packet $|\psi(0)\rangle$ is a superposition of a sufficient number of basis states, it is expected to revive at periodic intervals of time, though these intervals could be quite long in practice[7]. A full revival at time T is signaled by the fact that the autocorrelation function $|\langle\psi(0)|\psi(T)\rangle|^2$ returns to its initial value of unity.

In a generic nonlinear medium, for wave packets which are peaked sufficiently sharply in energy about some eigenvalue labeled by n_0 , we may expand the energy spectrum E_n in a Taylor series about E_{n_0} , and retain only terms up to the second order in $(n - n_0)$. It can then be shown[9] that fractional revivals of the wave packet occur at certain instants of time between successive revivals, when the wave packet splits into a superposition of a finite number of spatially separated sub-packets, each of which closely resembles the original one. This non-classical phenomenon arises due to very specific quantum interference properties between the basis states comprising the original wave packet[10]. The dynamics of a wave packet evolving in a Kerr-like medium is governed by the model Hamiltonian

$$H = \hbar\chi a^{\dagger 2} a^2 = \hbar\chi N(N - 1), \quad (1)$$

where $N = a^\dagger a$ and a, a^\dagger are photon annihilation and creation operators, so that $[a, a^\dagger] = 1$. The positive constant χ represents the susceptibility of the nonlinear medium. (The same Hamiltonian is applicable to a Bose-Einstein condensate propagating in a three-dimensional

*Electronic address: sudheesh,slbala,vbalki@physics.iitm.ac.in

optical lattice. In this case, a and a^\dagger are atom annihilation and creation operators, and χ characterizes the energy needed to overcome the inter-atomic repulsion.)

For ready reference, we first state the results[5] for an initial coherent state $|\psi(0)\rangle = |\alpha\rangle$, where $a|\alpha\rangle = \alpha|\alpha\rangle$ and the complex number $\alpha \equiv (x_0 + ip_0)/\sqrt{2}$ labels the CS. Such an initial state can be shown to revive periodically, with a revival time

$$T_{\text{rev}} = \pi/\chi. \quad (2)$$

Between $t = 0$ and $t = T_{\text{rev}}$, fractional revivals occur at times $t = \pi j/(k\chi)$, where $k = 2, 3, \dots$ and $j = 1, 2, \dots, (k-1)$ for a given value of k . At time $(j/k)T_{\text{rev}}$, the initial Gaussian wave packet splits into k spatially distributed sub-packets that are similar to itself. Full revivals of the wave packet can be discerned by observing the time evolution of the expectation values (first moments) of the operators $x \equiv (a + a^\dagger)/\sqrt{2}$ and $p \equiv (a - a^\dagger)/(i\sqrt{2})$, while distinctive signatures of the k -sub-packet fractional revivals manifest themselves in the temporal behavior of the k^{th} moments of x and p . The time dependence of all moments of x and p can be obtained from the general result

$$\begin{aligned} \langle a^{\dagger r} a^{r+s} \rangle &\equiv \langle \psi(t) | a^{\dagger r} a^{r+s} | \psi(t) \rangle \\ &= \alpha^s \nu^r e^{-\nu(1-\cos 2s\chi t)} \\ &\times e^{-i\chi[s(s-1)+2rs]t - i\nu \sin 2s\chi t}, \end{aligned} \quad (3)$$

where r and s are non-negative integers, and $\nu \equiv |\alpha|^2$ is the mean number of photons in the CS. Writing $\langle \psi(t) | x | \psi(t) \rangle = \langle x(t) \rangle$, etc., it is evident that $\langle x(0) \rangle = x_0$ and $\langle p(0) \rangle = p_0$. We find

$$\begin{aligned} \langle x(t) \rangle &= e^{-\nu(1-\cos 2\chi t)} [x_0 \cos(\nu \sin 2\chi t) \\ &+ p_0 \sin(\nu \sin 2\chi t)], \end{aligned} \quad (4)$$

with a similar expression for $\langle p(t) \rangle$. Owing to the exponential factor on the RHS we find that, for sufficiently large values of ν , $\langle x(t) \rangle$ remains essentially equal to $\langle x(0) \rangle$ for much of the time, except for significant and rapid variation near instants of full revival. This behavior is shared by $\langle p(t) \rangle$. A sudden change in $\langle x(t) \rangle$ or $\langle p(t) \rangle$ thus signals the occurrence of a revival of the initial wave packet. Similarly, writing $\langle \psi(t) | x^2 | \psi(t) \rangle = \langle x^2(t) \rangle$, we can show that

$$\begin{aligned} 2\langle x^2(t) \rangle &= 1 + x_0^2 + p_0^2 + e^{-\nu(1-\cos 4\chi t)} \\ &\times [(x_0^2 - p_0^2) \cos(2\chi t + \nu \sin 4\chi t) \\ &+ 2x_0 p_0 \sin(2\chi t + \nu \sin 4\chi t)]. \end{aligned} \quad (5)$$

Once again, for large values of ν , $\langle x^2(t) \rangle$ is more or less static around the value $\langle x^2(0) \rangle$ except at times close to $\pi/(2\chi) = \frac{1}{2}T_{\text{rev}}$, when the 2-sub-packet fractional revival occurs. Similar behavior is displayed by $\langle p^2(t) \rangle$. An explicit calculation reveals that, in general, the signature of a k -sub-packet fractional revival is mirrored in the dynamics of $\langle x^k(t) \rangle$ (equivalently, of $\langle p^k(t) \rangle$). It follows

that the plot of Δx (the standard deviation in x) versus Δp (the standard deviation in p) captures the occurrence of a 2-sub-packet fractional revival. Likewise, the square of the skewness in x (or p) mirrors the occurrence of a 3-sub-packet fractional revival, while the temporal behaviour of the kurtosis of x (or p) enables us to detect the appearance of a 4-sub-packet fractional revival.

Next, we turn to the case in which the initial state is a PACS rather than a (perfectly coherent) CS. The normalized m -photon-added coherent state $|\alpha, m\rangle$ ($m = 1, 2, \dots$) is defined as

$$|\alpha, m\rangle = \frac{(a^\dagger)^m |\alpha\rangle}{\sqrt{\langle \alpha | a^m a^{\dagger m} | \alpha \rangle}} = \frac{(a^\dagger)^m |\alpha\rangle}{\sqrt{m! L_m(-\nu)}}, \quad (6)$$

where L_m is the Laguerre polynomial of order m . The PACS just defined is also a *nonlinear* coherent state in the sense that it is an eigenstate of a nonlinear annihilation operator, namely,

$$\left(1 - \frac{m}{1 + a^\dagger a}\right) a |\alpha, m\rangle = \alpha |\alpha, m\rangle. \quad (7)$$

A PACS of this sort can be produced in laser-atom interactions under appropriate conditions[6]. Clearly, with increasing m (the number of photons ‘added’ to the ideal CS $|\alpha\rangle$), there is increasing departure from perfect coherence. It is straightforward to see that, when an initial state $|\alpha, m\rangle$ evolves under the Hamiltonian in Eq. (1), revivals and fractional revivals of the wave packet occur at the same instants as in the case of a coherent initial state, and that their appearance is mirrored in the time evolution of the expectation values of the different moments of the quadratures x and p , as before. However, the actual dynamics of these expectation values is much more complex, even for small values of m : even a small departure from Poisson number statistics in the initial state leads to significant changes in the evolution of the wave packet.

To illustrate this explicitly, we find first the counterpart of Eq. (3) for the general initial state $|\psi(0)\rangle = |\alpha, m\rangle$. The result can be written in closed form as

$$\begin{aligned} \langle a^{\dagger r} a^{r+s} \rangle_m &= \alpha^s e^{-\nu + \nu \cos 2s\chi t - i\chi(s-1+2m)st - i\nu \sin 2s\chi t} \\ &\times \sum_{n=0}^r \binom{r}{n} \frac{m! (\nu e^{-2is\chi t})^n L_m^{s+n}(-\nu e^{-2is\chi t})}{(m-r+n)! L_m(-\nu)}, \end{aligned} \quad (8)$$

where L_m^n denotes the associated Laguerre polynomial. Setting $m = 0$, we recover Eq. (3) for an initial state $|\alpha\rangle$. For an initial state $|\alpha, 1\rangle$, corresponding to minimal departure from coherence in this class of PACS, we set $r = 0$, $s = 1$ and $m = 1$ in Eq. (8) to obtain the expectation value of $a(t)$, and hence the expectation value of $x(t)$, denoted by $\langle x(t) \rangle_1$. We get

$$\langle x(t) \rangle_1 = e^{-\nu(1-\cos 2\chi t)} [x_0 \text{Re } z_1(t) + p_0 \text{Im } z_1(t)], \quad (9)$$

where

$$z_1 = \left(\frac{2 + \nu e^{2i\chi t}}{1 + \nu} \right) e^{i(2\chi t + \nu \sin 2\chi t)}. \quad (10)$$

Similarly, for the initial state $|\alpha, 2\rangle$ we find

$$\langle x(t) \rangle_2 = e^{-\nu(1-\cos 2\chi t)} [x_0 \operatorname{Re} z_2(t) + p_0 \operatorname{Im} z_2(t)], \quad (11)$$

where

$$z_2 = \left(\frac{6 + 6\nu e^{2i\chi t} + \nu^2 e^{4i\chi t}}{2 + 4\nu + \nu^2} \right) e^{i(4\chi t + \nu \sin 2\chi t)}. \quad (12)$$

It is evident that these expressions are already considerably more involved than that in Eq. (4) for $m = 0$. In particular, we note the occurrence, in the exponents, of secular terms in t apart from sinusoidal terms involving higher harmonics. Similar remarks apply to the expectation value of p in these cases. The time-dependence of the higher moments of x and p are even more involved. We do not go into these here.

In general, the effects of the departure from coherence of the initial wave packet on its subsequent dynamics are not significant if $\nu \gg m$, since the overall exponential factor $\exp[-\nu(1-\cos 2\chi t)]$ ensures that the expectation values are essentially static except for sudden changes at times close to revivals and fractional revivals. This is not valid for smaller values of ν . In particular, squeezing and higher-order squeezing effects depend crucially on the precise nature of the initial state, as we shall now see.

III. SQUEEZING AND HIGHER-ORDER SQUEEZING

We begin by summarizing the condition for q^{th} -power amplitude-squeezing of a quantum state and outlining the squeezing properties exhibited by an initial CS as it propagates through a Kerr-like medium[4]. We then examine in detail the squeezing properties exhibited by an initial PACS as it evolves in the medium, and compare its behavior with that of a CS.

One first defines the two quadrature variables

$$Z_1 = \frac{(a^q + a^{\dagger q})}{\sqrt{2}}, \quad Z_2 = \frac{(a^q - a^{\dagger q})}{i\sqrt{2}} \quad (q = 1, 2, 3, \dots). \quad (13)$$

The generalized uncertainty principle gives

$$(\Delta Z_1)^2 (\Delta Z_2)^2 \geq \frac{1}{4} |\langle [Z_1, Z_2] \rangle|^2, \quad (14)$$

where ΔZ_i is the standard deviation of Z_i , and the expectation values refer to those in the state concerned. The state is said to be q^{th} -power amplitude-squeezed in the variable Z_1 if

$$(\Delta Z_1)^2 < \frac{1}{2} |\langle [Z_1, Z_2] \rangle|. \quad (15)$$

Amplitude squeezing in Z_2 is similarly defined. We write $[a^q, a^{\dagger q}] = F_q(N)$ (this is a certain polynomial of order $(q-1)$ in the number operator N) and define the quantity

$$D_q(t) = \frac{(\Delta Z_1)^2 - \frac{1}{2} \langle F_q(N) \rangle}{\frac{1}{2} \langle F_q(N) \rangle}, \quad (16)$$

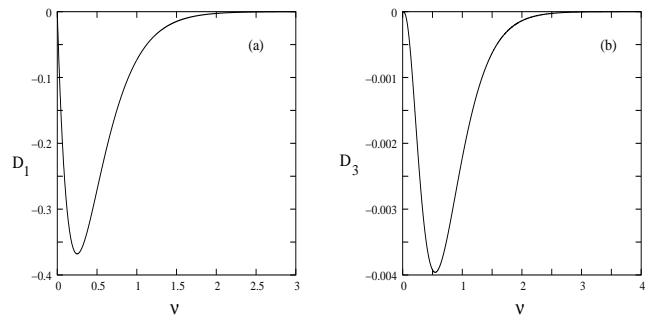


FIG. 1: Plots of $D_q(\frac{1}{2}T_{\text{rev}})$ versus ν for an initial CS (with $\theta = 0$), for (a) $q = 1$ and (b) $q = 3$. (Note the different ordinate scales in the two cases.)

where the time-dependence has been indicated explicitly to remind us that the expectation values involved are those in the instantaneous state of the system. It is easily seen that the state is q^{th} -power amplitude-squeezed in Z_1 if $-1 \leq D_q < 0$. We can rewrite Eq. (16) in terms of a^q and $a^{\dagger q}$ as

$$D_q(t) = \frac{2 \left[\operatorname{Re} \langle a^{2q} \rangle - 2 (\operatorname{Re} \langle a^q \rangle)^2 + \langle a^{\dagger q} a^q \rangle \right]}{\langle F_q(N) \rangle}. \quad (17)$$

When the initial state is the CS $|\alpha\rangle$, the (time-dependent) expectation values on the RHS can be evaluated[4] using Eq. (3).

We are interested, in particular, in examining whether fractional revivals are accompanied by any significant degree of squeezing and higher-order squeezing. For this purpose, we focus on $D_q(t)$ at the instant $t = \pi/(2\chi) = \frac{1}{2}T_{\text{rev}}$, corresponding to a 2-sub-packet fractional revival. After simplification, we find that D_q vanishes at this instant for all even values of q , implying that no even-order squeezing of the state accompanies this fractional revival. For odd values of q , however, we find

$$D_q(T_{\text{rev}}/2) = \frac{2\nu^q}{\langle F_q(N) \rangle} (\sin^2 q\theta - e^{-4\nu} \cos^2 q\theta), \quad (18)$$

where θ is the argument of $\alpha (= \nu^{1/2} e^{i\theta})$. Thus squeezing (or higher-order squeezing) occurs at this instant provided $D_q < 0$, i.e., $|\tan q\theta| < e^{-2\nu}$. We illustrate this in Figs. 1(a) and (b), where D_1 and D_3 are plotted as functions of ν for an initial CS with $\theta = 0$. (We have set $\chi = 5$ in all the numerical results presented in this paper.) We have also plotted D_1 and D_3 as functions of θ for a fixed value of $\nu (= 0.1)$ in Figs. 2(a) and (b), showing how squeezing occurs for certain ranges of the argument of α , when D_q becomes negative.

We now show that if the initial state departs even marginally from coherence, as in a PACS with a small value of m , these results change significantly. Writing D_q as $D_q^{(m)}$ when the expectation values in Eq. (17) are evaluated for an initial state $|\alpha, m\rangle$, we find the following general result: setting $A = \frac{1}{2}L_m(-\nu) \langle F_q(N) \rangle$, we have

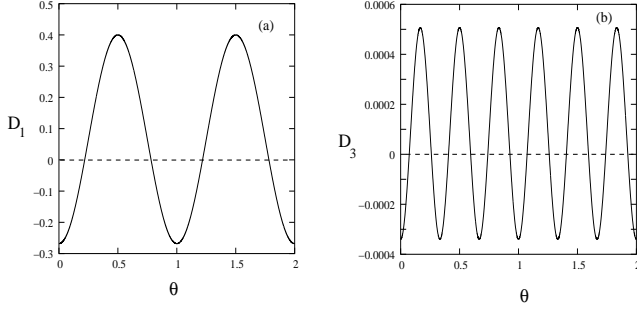


FIG. 2: Plots of $D_q(\frac{1}{2}T_{\text{rev}})$ versus θ for an initial CS (with $\nu = 0.1$), for (a) $q = 1$ and (b) $q = 3$.

$$\begin{aligned}
 AD_q^{(m)}(t) = & e^{-\nu(1-\cos 4\chi qt)} \sum_{n=0}^m \binom{m+2q}{n+2q} \frac{\nu^{n+q}}{n!} \cos \left(2(2m+2n+q-1)\chi qt + \nu \sin 4\chi qt - 2q\theta \right) \\
 & - \frac{2e^{-2\nu(1-\cos 2\chi qt)}}{L_m(-\nu)} \left\{ \sum_{n=0}^m \binom{l+q}{n+q} \frac{\nu^{n+q}}{n!} \cos \left((q-1+2m+2n)\chi qt + \nu \sin 2\chi qt - q\theta \right) \right\}^2 \\
 & + \sum_{n=n_{\min}}^q \binom{q}{n} \frac{m!}{(m-q+n)!} \nu^n L_m^n(-\nu), \tag{19}
 \end{aligned}$$

where $n_{\min} = \text{Max}(0, q - m)$. This generalizes the expression for D_q obtained[4] for a coherent state, which corresponds to $m = 0$.

As before, we examine $D_q^{(m)}$ at $t = \pi/(2\chi)$ for the possibility of squeezing and higher-order squeezing. The foregoing expression reduces at this instant of time to

$$\begin{aligned}
 AD_q^{(m)}(T_{\text{rev}}/2) = & (-\nu)^q L_m^{2q}(-\nu) \cos 2q\theta \\
 & - \frac{2e^{-2\nu(1-\cos q\pi)}}{L_m(-\nu)} \nu^q \left\{ L_m^q((-1)^q \nu) \right\}^2 \cos^2 q\theta \\
 & + \sum_{n=n_{\min}}^q \binom{q}{n} \frac{m!}{(m-q+n)!} \nu^n L_m^n(-\nu). \tag{20}
 \end{aligned}$$

We use this to analyze various cases numerically. In contrast to what happens for an initial CS, it turns out that there is no *odd*-power amplitude-squeezing for an initial PACS. Even-power amplitude-squeezing does occur, though, for sufficiently large values of ν . This is illustrated in Figs. 3(a) and (b), which show the range of ν for which D_2 falls below zero. Figures 4(a) and (b) depict the variation of D_2 with the phase angle θ for a fixed value of ν .

Turning to the extent of squeezing as a function of time, Fig. 5 compares the temporal variation of the standard deviation Δx for an initial CS ($m = 0$) and an initial PACS ($m = 1$), with $\alpha = 1$ (hence $\theta = 0$). The horizontal dashed line demarcates the level below which the state is squeezed. It is evident that squeezing in the rigorous sense accompanies the fractional revival

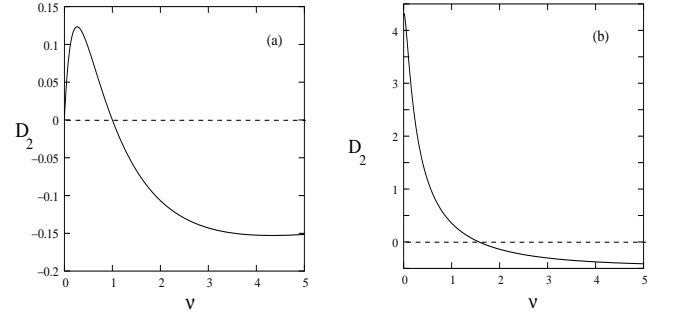


FIG. 3: Plots of $D_2(\frac{1}{2}T_{\text{rev}})$ versus ν (with $\theta = 0$), for an initial PACS with (a) $m = 1$ and (b) $m = 10$.

at $t = \frac{1}{2}T_{\text{rev}}$ when the initial state is a CS. This feature is suppressed when it is a PACS, although Δx does dip down considerably around this fractional revival.

We have focused on q^{th} -power amplitude-squeezing at fractional revivals, as this turns out to provide rather more discriminatory signatures of higher-order squeezing effects than the other alternative, namely, Hong-Mandel squeezing[11]. However, a few remarks on the latter are in order here. The relevant variables in the case of Hong-Mandel squeezing are $(a + a^\dagger)^q/\sqrt{2}$ and $(a - a^\dagger)^q/(i\sqrt{2})$, i.e., essentially the q^{th} powers of x and p . For $q = 1$, of course, Hong-Mandel squeezing is the same as amplitude-squeezing, but the two kinds of squeezing differ for $q \geq 2$. Figs. 6(a) and (b) show how $\langle (x - \langle x \rangle)^4 \rangle$, the fourth moment of x about its mean value, varies over a revival

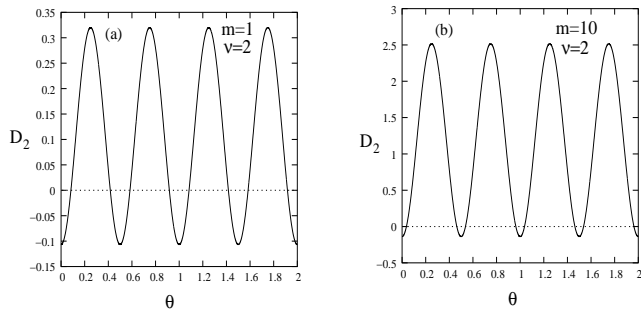


FIG. 4: Plots of $D_2(\frac{1}{2}T_{\text{rev}})$ versus θ (with $\nu = 2$), for an initial PACS with (a) $m = 1$ and (b) $m = 10$.

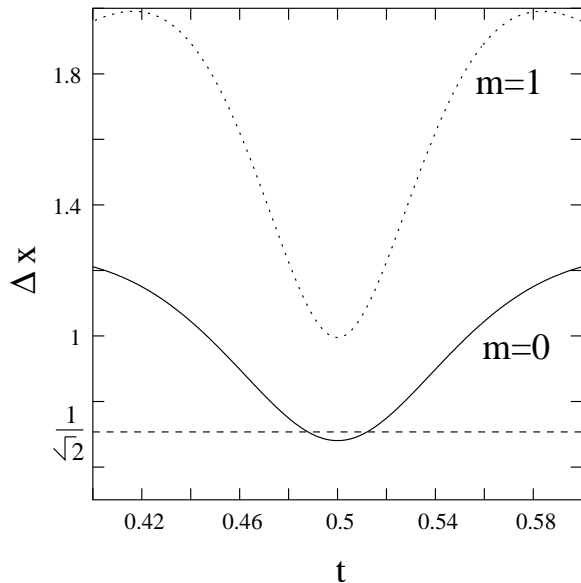


FIG. 5: Δx versus time in units of T_{rev} , in the case $x_0 = \sqrt{2}$, $p_0 = 0$.

period for an initial CS and PACS, respectively. The horizontal dotted lines indicate the bound on $\langle (x - \langle x \rangle)^4 \rangle$, below which fourth-order Hong-Mandel squeezing occurs in this quadrature. An initial CS exhibits such squeezing near revivals, and comes close to doing so near the fractional revival at $\frac{1}{2}T_{\text{rev}}$, but does not actually do so. An initial PACS does not display such higher-order squeezing at any time, although $\langle (x - \langle x \rangle)^4 \rangle$ attains its lowest value at revival times. However, fractional revivals are marked by rapid oscillations of $\langle (x - \langle x \rangle)^4 \rangle$, these being most pronounced around the 2-sub-packet fractional revival. These features are enhanced further in the case of initial states with larger values of m .

IV. THE WIGNER FUNCTION AND THE NON-CLASSICALITY INDICATOR

Finally, we examine the Wigner functions corresponding to the wave packets at instants of fractional revivals,

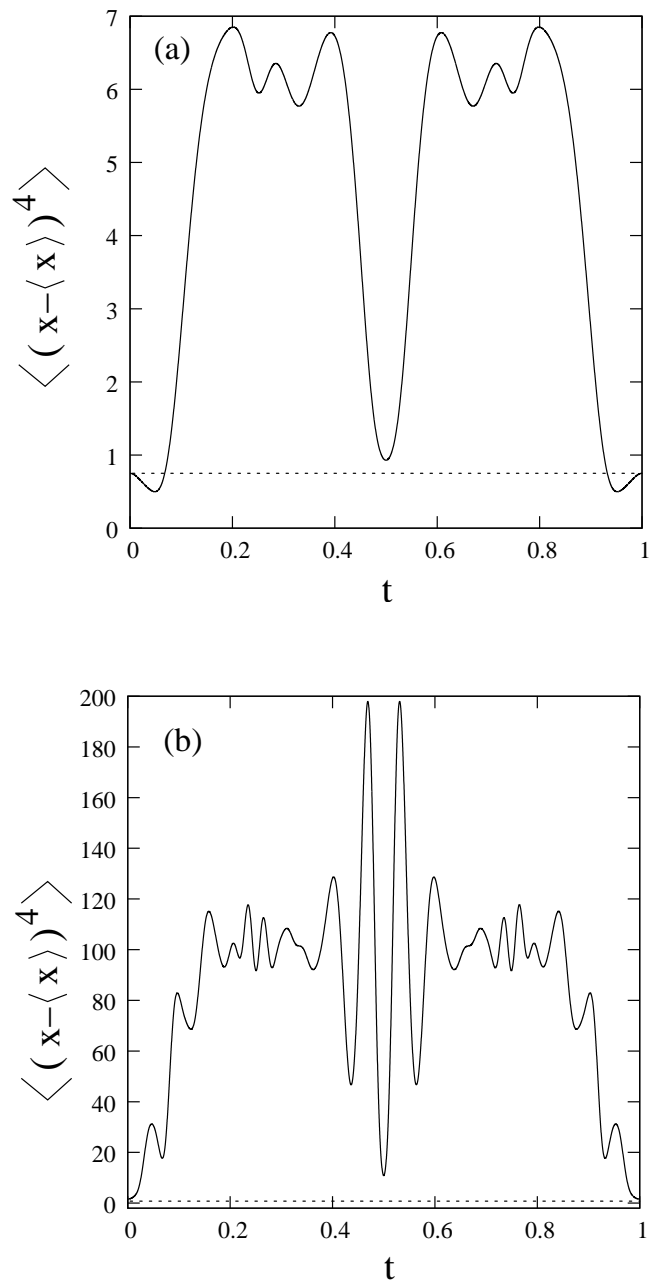


FIG. 6: Plots of $\langle (x - \langle x \rangle)^4 \rangle$ versus time in units of T_{rev} for initial states (a) $|\alpha\rangle$ and (b) $|\alpha, 5\rangle$, with $\nu = 1$. Note the very different ordinate scales in the two cases.

to quantify non-classical behavior during their time evolution. It is well known that the “extent” to which the Wigner function becomes negative (as a function of its complex argument) is an indicator of the non-classicality of the state concerned. The normalized Wigner function

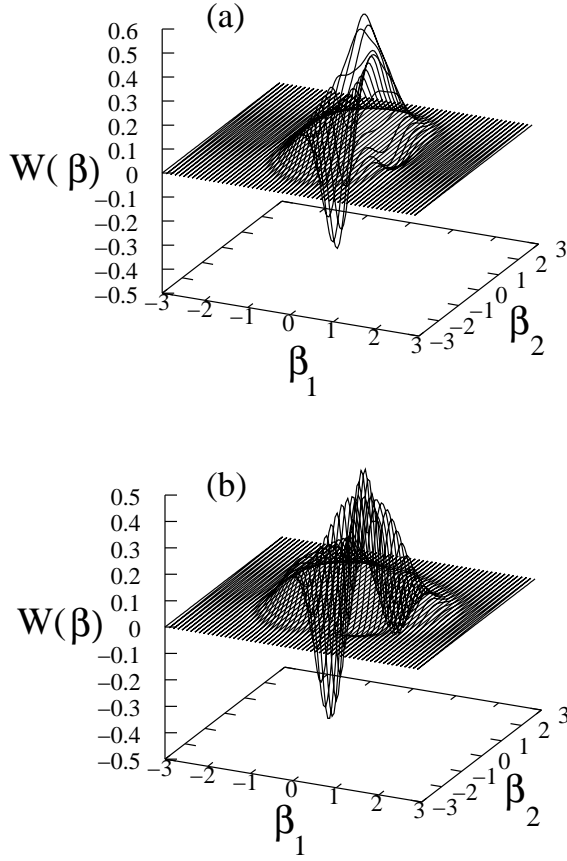


FIG. 7: Plots of the Wigner function corresponding to an initial state $|\alpha\rangle$ with $\alpha = 1$, at (a) $t = \frac{1}{2}T_{\text{rev}}$ and (b) $t = \frac{1}{3}T_{\text{rev}}$. Here, and in the succeeding figures, $\beta_1 = \text{Re } \beta$, $\beta_2 = \text{Im } \beta$.

$W(\beta; t)$ (where $\beta \in \mathbb{C}$) is given by[12]

$$W(\beta; t) = \frac{2}{\pi} e^{-2|\beta|^2} \text{Re} \left\{ \sum_{\substack{l, n=m \\ n \geq l}}^{\infty} (-1)^l (2 - \delta_{ln}) (l!/n!)^{1/2} \right. \\ \left. \times (2\beta)^{n-l} \rho_{ln}(t) L_l^{n-l}(4|\beta|^2) \right\}, \quad (21)$$

where $\rho_{ln}(t)$ is the density matrix element corresponding to the state at time t in the oscillator Fock basis. For an initial coherent state $|\alpha\rangle$ we have the standard result

$$\rho_{ln}(0) = \frac{\alpha^{*n} \alpha^l}{\sqrt{l! n!}} e^{-|\alpha|^2}, \quad (22)$$

leading to the well-known expression

$$W(\beta; 0) = \frac{2}{\pi} e^{-2|\alpha - \beta|^2}. \quad (23)$$

for the Wigner function. This is positive definite everywhere in the complex β -plane, justifying the appellation “classical” for an oscillator coherent state $|\alpha\rangle$. The time evolution of the Wigner function under the Hamiltonian of Eq. (1) may be computed readily using the representation $\rho(t) = \sum_{l, n=0}^{\infty} \rho_{ln}(t) |l\rangle \langle n|$ for the density matrix.

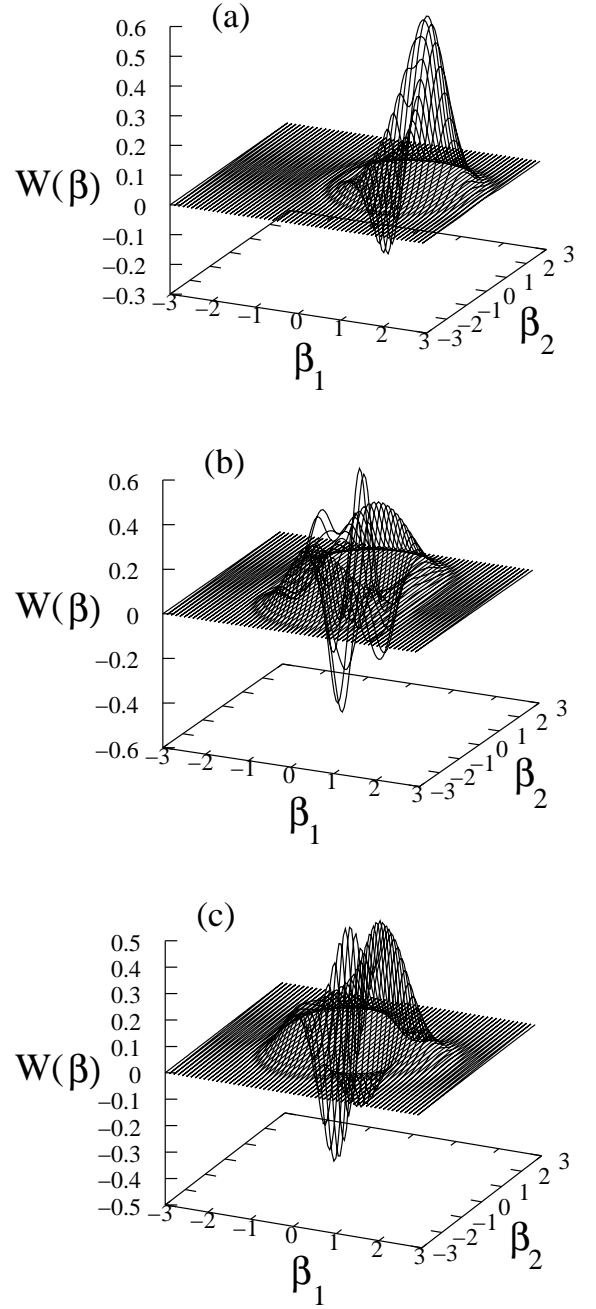


FIG. 8: Plots of the Wigner function corresponding to an initial state $|\alpha, 1\rangle$ with $\alpha = 1$, at (a) $t = 0$, (b) $t = \frac{1}{2}T_{\text{rev}}$ and (c) $t = \frac{1}{3}T_{\text{rev}}$.

Figures 7(a) and (b) show how the Wigner function for this initial CS behaves at the instants of the 2-sub-packet and 3-sub-packet fractional revivals, respectively.

For the initial photon-added coherent state $|\alpha, m\rangle$, one finds[6]

$$\rho_{ln}(0) = \frac{e^{-\nu}}{m! L_m(-\nu)} \frac{\alpha^{l-m} \alpha^{*n-m} \sqrt{l! n!}}{(l-m)! (n-m)!}. \quad (24)$$

Correspondingly, the Wigner function at $t = 0$ can be

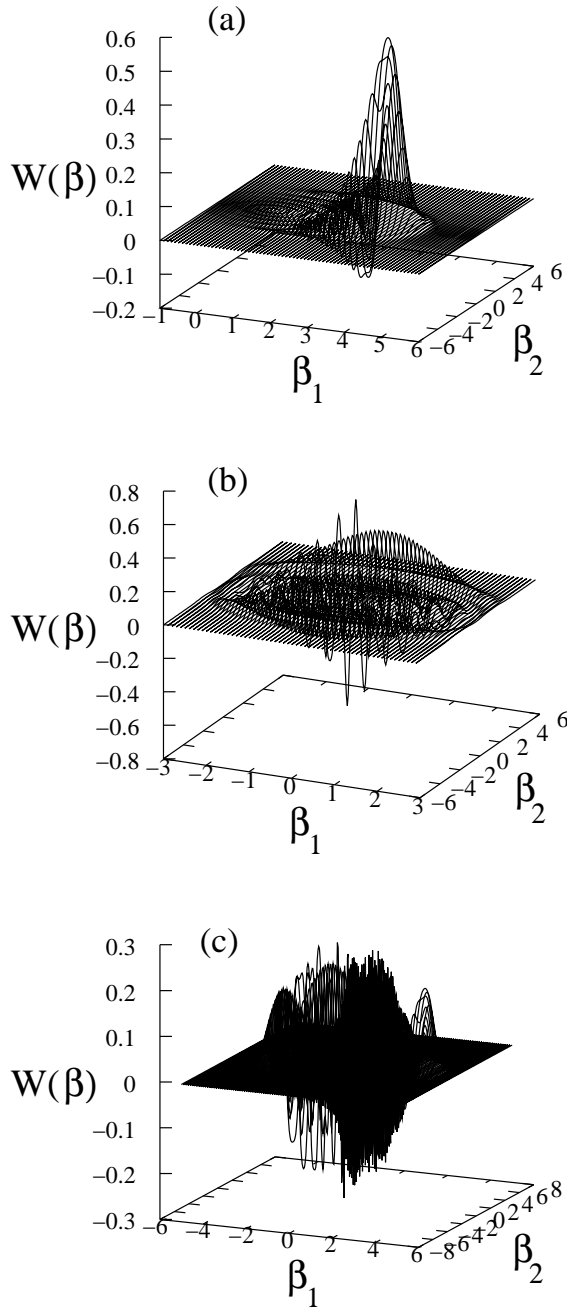


FIG. 9: Plots of the Wigner function corresponding to an initial state $|\alpha, 10\rangle$ at (a) $t = 0$, (b) $t = \frac{1}{2}T_{\text{rev}}$ and (c) $t = \frac{1}{3}T_{\text{rev}}$.

expressed in the closed form

$$W(\beta; 0) = \frac{2(-1)^m}{\pi L_m(-\nu)} L_m(|2\beta - \alpha|^2) e^{-2|\alpha - \beta|^2}. \quad (25)$$

It is to be noted that this is no longer positive definite for all complex β , reflecting the fact that this initial state is no longer “totally” classical, as it departs from perfect coherence by the photons that have been “added” to $|\alpha\rangle$ to

produce the PACS. Figures 8(a), (b) and (c) are plots of

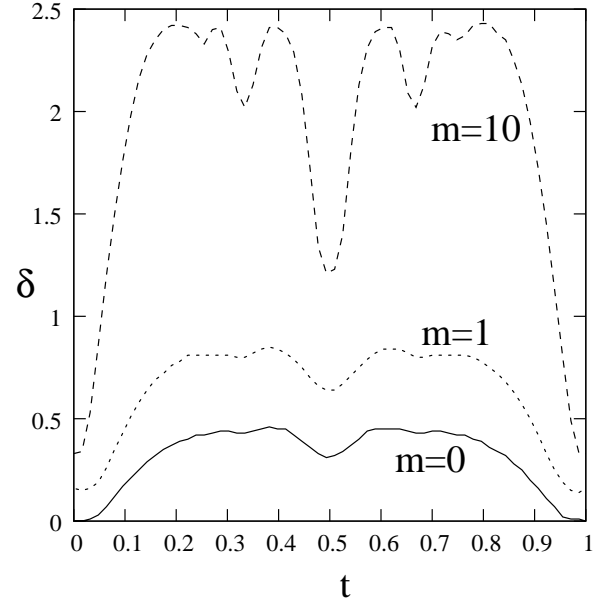


FIG. 10: Plot of δ versus time in units of T_{rev} .

$W(\beta; t)$ for the case $m = 1$ at $t = 0$, $\frac{1}{2}T_{\text{rev}}$ and $\frac{1}{3}T_{\text{rev}}$, respectively. The corresponding plots for the case $m = 10$ are shown in Figs. 9(a), (b) and (c). With increasing m , the oscillations of the Wigner function in the β -plane between positive and negative values become more pronounced, and the region of non-classicality becomes more extensive.

To get an idea of the degree of non-classicality as a continuously varying function of time for each of the different initial states we have considered, it is instructive to consider the non-negative quantity δ defined as[13]

$$\begin{aligned} \delta(t) &= \int d^2\beta (|W(\beta; t)| - W(\beta; t)) \\ &= \int d^2\beta |W(\beta; t)| - 1. \end{aligned} \quad (26)$$

The larger the value of δ , the greater is the extent of non-classicality of the state concerned, although of course δ alone does not give a complete picture of the oscillations of the Wigner function. In Fig. 10 we have plotted δ versus t for initial states $|\alpha\rangle$, $|\alpha, 1\rangle$, and $|\alpha, 10\rangle$ where α has been set equal to unity. It is clear that in the interval between $t = 0$ and $t = T_{\text{rev}}$, δ is least at the 2-sub-packet fractional revival, followed by its values at the 3-sub-packet and 4-sub-packet fractional revivals. This feature becomes increasingly prominent for larger values of m , showing that the extent of non-classicality also increases with m , as expected.

This work was supported in part by the Department of Science and Technology, India, under Project No. SP/S2/K-14/2000.

-
- [1] See, for instance, S. L. Braunstein and A. K. Pati, *Quantum Information with Continuous Variables* (Kluwer, Dordrecht, 2003).
- [2] See, for instance, V. V. Dodonov, *J. Opt. B: Quant. Semiclass. Opt.* **4**, R1 (2002).
- [3] See, for instance, R. W. Robinett, *Phys. Rep.* **392**, 1 (2004).
- [4] S. D. Du and C. D. Gong, *Phys. Rev. A* **48**, 2198 (1993).
- [5] C. Sudheesh, S. Lakshmi, and V. Balakrishnan, *Phys. Lett. A* **329**, 14 (2004).
- [6] G.S. Agarwal and K. Tara, *Phys. Rev. A* **43**, 492 (1991).
- [7] V. P. Gutschick and M. M. Nieto, *Phys. Rev. D* **22**, 403 (1980).
- [8] B. Yurke and D. Stoler, *Phys. Rev. Lett.* **57**, 13 (1986); G. J. Milburn and C. A. Holmes, *ibid.* **56**, 2237 (1986); W. Schleich, M. Pernigo, and F. L. Kien, *Phys. Rev. A* **44**, 2172 (1991); V. Buzek, H. Moya-Cessa, P. L. Knight, and S. J. D. Phoenix, *ibid.* **45**, 8190 (1992).
- [9] I. Sh. Averbukh and N. F. Perelman, *Phys. Lett. A* **139**, 449 (1989); *Acta. Phys. Pol.* **78**, 33 (1990).
- [10] K. Tara, G. S. Agarwal, and S. Chaturvedi, *Phys. Rev. A* **47**, 5024 (1993).
- [11] C. K. Hong and L. Mandel, *Phys. Rev. Lett.* **54**, 323 (1985).
- [12] M. Brune, S. Haroche, J. M. Raimond, L. Davidovich, and N. Zagury, *Phys. Rev. A* **45**, 5193 (1992).
- [13] A. Kenfack and K. Zyczkowski, *J. Opt. B: Quant. Semiclass. Opt.* **6**, 396 (2004).